Progress In Electromagnetics Research C, Vol. 36, 57–67, 2013

NOVEL COMPACT MULTILAYER CROSS-COUPLED FILTER WITH ENHANCED INNER COUPLING SCHEME

Wei Tang* **and Xiaobo Yang**

Research Institute of Electronic Science and Technology, University of Electronic Science and Technology of China, Chengdu 611731, China

Abstract—A novel cross-coupled resonator filter with multilayer structure is presented in this paper. By using enhanced inner coupling structure and 3D layout, the resonator size is largely reduced, and high spurious frequency could be achieved. To validate the proposed topology, a cross-coupled 3D filter with inner coupling capacitor is easily fabricated on a normal printed circuit board. The measured results show the characteristics of small size, good stopband performance and high spurious frequency.

1. INTRODUCTION

As one of the key components in modern wireless communication and measuring systems, filters with compact size, low cost, high reliability and good performance has attracted much attention in recent years. In order to reduce the size of the planar filter without sacrificing performance, many techniques have been reported in the literature. For instance, some of the filter configurations use hairpin resonator [1–4], step impedance resonator (SIR) [5–9], ring resonator [10–14], short circuited stub [15–17], and defected ground structure [18, 19].

Among various planar filter configurations, SIR filters have become a hot topic because of their ability to reduce the circuit size and improve the upper stopband performance. SIR filters with parallel-coupled structure are commonly used [5, 6], but their size seems still large. To relieve this problem, several filter designs utilizing folded quarter-wavelength stepped-impedance resonators have been reported [7, 8]. The occupied area of coupled-resonator pair may be

Received 21 November 2012, Accepted 26 December 2012, Scheduled 4 January 2013
* Corresponding author: Wei Tang (tangwei@uestc.edu.cn).

reduced, but since the short stubs of the quarter-wavelength SIR are grounded through via holes, their parasitic effect could not be easily controlled especially in high frequency. SIR bandpass filter with defected ground structure (DGS) and electromagnetic bandgap (EBG) structure are proposed in [26, 27]. Moreover, various kinds of SIR bandpass filters with high performance are presented in [29–32], but their sizes are not small compared with the structure in this design.

Low Temperature Co-fired Ceramics (LTCC) is a suitable technological solution for further miniaturization of SIR filters because of its three-dimensional structure and outstanding electrical properties. More, it is easy to integrate various passive elements with compact size and low production costs. SIR filters based on LTCC in [20, 21, 28] have small size and excellent performance, but their structures are complicated thus require high fabrication precision.

By using a multilayer structure, the resonator has advantages of compact size and simple fabrication process. The paper presents a cross-coupled filter with multilayer structure. By introducing inner coupling capacitor, the filter size is largely miniaturized and the Q value is improved. Thus the filter has the merits of small size(about $0.17\lambda_g \times 0.06\lambda_g$), high spurious suppression and easy integration. Several contents are illustrated as below. First of all, the meandered 3D structured resonator is proposed to realize a compact size with little parasitic effect. Then, by tuning the distance between the two electrodes of a resonator, the inner coupling could be adjusted to achieve a proper resonant frequency and bandwidth. Besides, the whole structure could be fabricated on a normal printed circuit board with good tolerance precision. Finally, a cross-coupled filter with inner coupling 3D structure is designed based on cross coupling theory and simulated coefficients. Good agreement between measured and simulated results is obtained.

2. MULTILAYER STRUCTURE RESONATOR DESIGN

$\lambda_g/4$ and $\lambda_g/2$-type SIR are widely used in most resonator filter applications, and the arms of $\lambda_g/2$-type SIR are always folded to realize a compact size, as shown in Fig. 1. More, the coupling between the two lines can further minimize the area.

$\lambda_g/2$ resonator can be viewed as a combination of coupled lines and a single microstrip. As shown in Fig. 1, the parallel-coupled line section has an electrical length θ_c and a pair of odd- and even-mode impedances denoted by Z_{co} and Z_{ce}, the electrical length of the single line is defined by $2\theta_o$. Based on the symmetrical structure, it can be analyzed by even-odd-method, thus the coupling coefficient of the

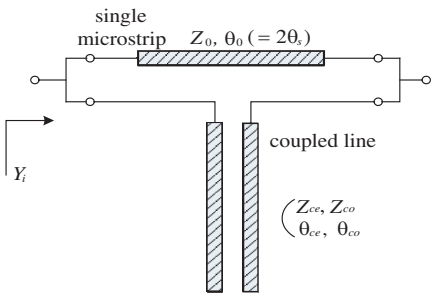

Figure 1. SIR model.

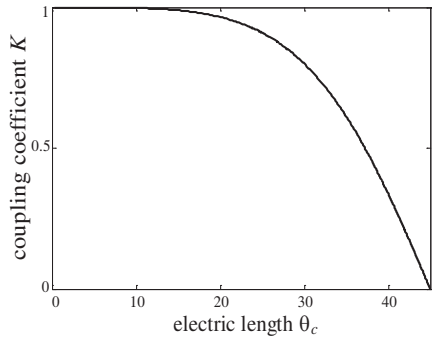

Figure 2. Coupling coefficient varying with electric length of resonator.

coupled line section is deduced as:

$$k \equiv (Z_{ce} - Z_{co})/(Z_{ce} + Z_{co}) \tag{1}$$

The resonance condition can be derived from:

$$\sqrt{1-k^2} \cdot (R_c/\tan\theta_c - \tan\theta_c/R_c) \cdot \sin 2\theta_o + 2\cos 2\theta_o - 2k = 0 \tag{2}$$

where $R_c = Z_c/Z_o$ is the impedance ratio of coupled line section and single microstrip.

According to Equation (2), the resonance condition depends on four independent factors, which are coupling coefficient k, impedance ratio R_c, electrical length θ_o and θ_c. Assume that $\theta_o = \theta_c$ and $R_c = 1.5$, the relation between k and $4\theta_o$ is illustrated in Fig. 2. As can be seen, the greater the coefficient is, the smaller the electrical length will be.

To increase the inner coupling and compact resonator size further, multilayer circuit structure is adopted in this design. As shown in Fig. 3, the SIR cell is folded in two layers with an inner coupling capacitor composed of upper and lower electrode pattern, which has an effect on resonance frequency. The low-impedance part has a length of 3.1 mm and a width of 2 mm, while the high-impedance part has a length of 7.8 mm and a width of 0.3 mm. Fig. 3 displays the resonance frequency varying with the thickness of substrate simulated by High-Frequency-Structure-Simulation (HFSS). Rogers 4350B is adopted here with a dielectric constant of 3.5. It can be seen that the resonance frequency rises from 1.18 GHz to 2.45 GHz when the distance t increases from 40 μm to 260 μm. The inner coupling capacitance decreases with the increment of substrate thickness, meanwhile the resonance frequency rises.

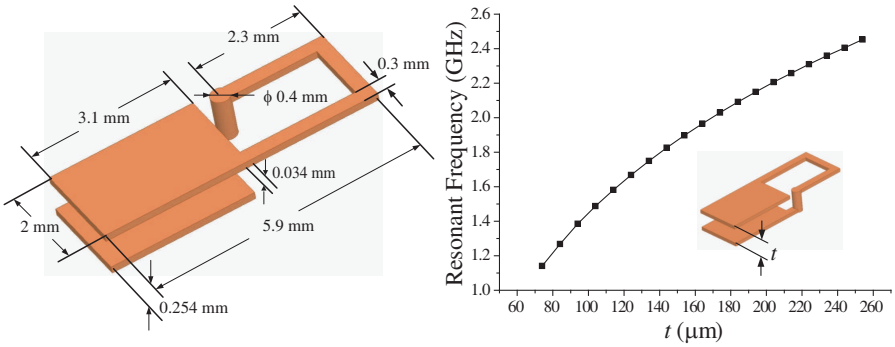

Figure 3. Resonance frequency of multilayered resonator against various distances t.

3. MULTILAYER CROSS-COUPLED FILTER DESIGN

General coupling matrix synthesis method is used in most cross-coupled filters design [22–25]. First, the transfer polynomial of the filter is obtained by specified center frequency, bandwidth, reflection response and locations of transmission zeros. Then the coupling matrix is deduced by method of residues and the unrealizable elements can be annihilated by applying a series of similarity transforms. Further, the detailed size and topology of the resonators are obtained by coupling matrix and filter structure. Finally, by fine tuning the dimensions of the resonator, the needed response curve of the filter could be realized based on HFSS simulation.

To demonstrate the practicability of the vertical coupling structure, a four-pole cross-coupled filter was designed with a center frequency of 2450 MHz and a bandwidth of 100 MHz. Cross-coupling was introduced between resonators 1 and 4, thus two transmission zeros of 2350 MHz and 2650 MHz could be realized. The corresponding matrix M and Q value were calculated by using a homemade MATLAB program, based on general coupling matrix synthesis method:

$$M = \begin{bmatrix} 0 & 0.0412 & 0 & -0.0114 \\ 0.0412 & 0 & 0.0373 & 0 \\ 0 & 0.0373 & 0 & 0.0412 \\ -0.0114 & 0 & 0.0412 & 0 \end{bmatrix} \tag{3}$$

$$Q = 20.5$$

In a general planar circuit, coupling factors are mainly decided by the horizontal distance between resonators. While in a 3D structure, the thickness of resonator electrode also has an effect on coupling coefficient.

Figure 4 illustrates the simulated electric coupling coefficients against different distance s and thickness t of the resonators. Be similar to single layer structure, electric coupling coefficient decreases with the increment of distance and rises with the increment of thickness. Besides, it should be noticed that the greater the thickness is, the higher the resonance frequency is. When coupling coefficients are simulated under different value of "s", the t is fixed as 0.254 mm. Similarly, when coupling coefficients are simulated under various value

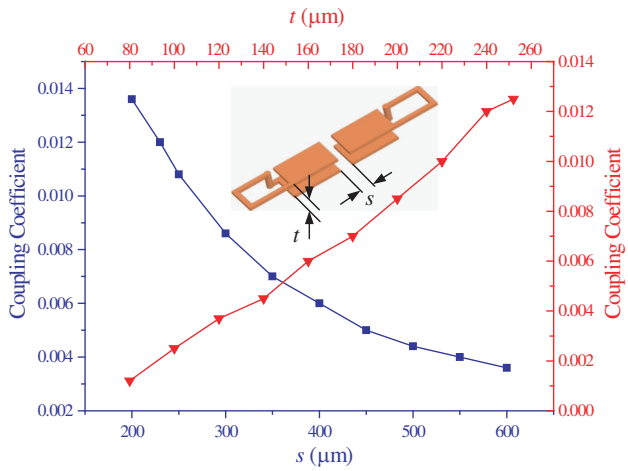

Figure 4. Electric coupling coefficients against different t and s.

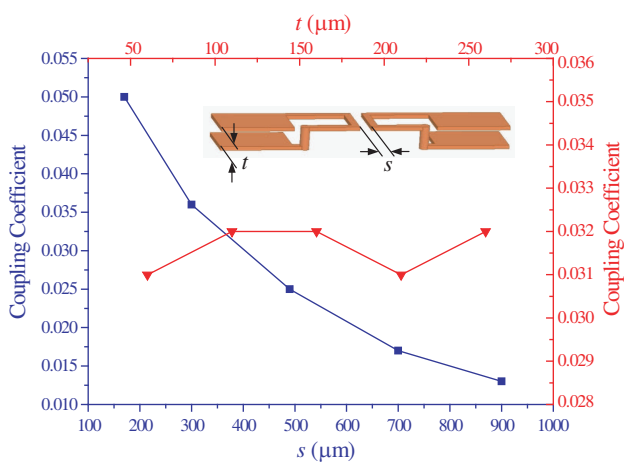

Figure 5. Magnetic coupling coefficients against different t and s.

of "t", the s is fixed as 0.3 mm. Moreover, it can be concluded that the coupling coefficient between resonator 1 and 4 reaches 0.0114 when $t = 0.254$ mm and $s = 0.26$ mm.

Similarly, the simulated magnetic coupling coefficients against different distances s and thicknesses t of the resonators are displayed in Fig. 5. It can be seen that magnetic coupling coefficient decreases with the increment of distance while changes a little when thickness increases from 100–900 μm. Because the magnetic coupling coefficient is mainly affected by resonators of the same layer, thus thickness has very little influence on magnetic coupling coefficient. When coupling coefficients are simulated under different value of "s", the t is fixed as 0.254 mm. Similarly, when coupling coefficients are simulated under various value of "t", the s is fixed as 0.5 mm. Besides, it is shown that the coupling coefficient between resonator 2 and 3 reaches 0.0114 when $t = 0.254$ mm and $s = 0.26$ mm.

When the thickness is fixed, mixed coupling coefficient varying with distance is shown in Fig. 6, meanwhile it illustrates mixed coupling coefficient varying with thickness where distance is fixed. Be similar to electric coupling coefficient, mixed coupling coefficient decreases with the increment of distance and rises with the increment of thickness. When coupling coefficients are simulated under different value of "s", the t is fixed as 0.254 mm. Similarly, when coupling coefficients are simulated under various value of "t", the s is fixed as 0.5 mm. Besides, it is illustrated that the coupling coefficient between resonator 1 and 2 achieves 0.0114 when $t = 0.254$ mm and $s = 0.26$ mm.

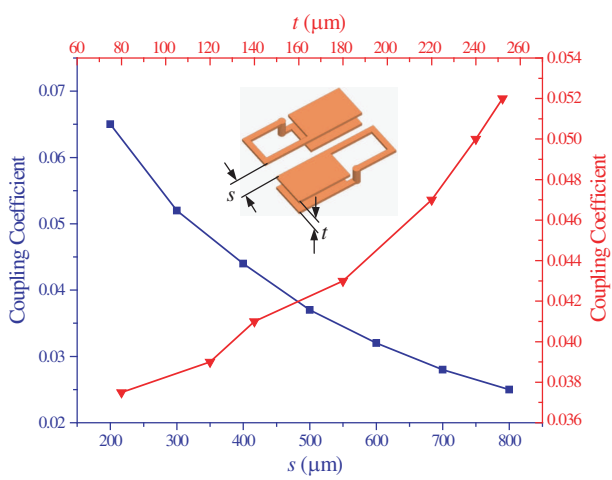

Figure 6. Mixed coupling coefficients against different t and s.

Finally, the S-parameter of the filter could be achieved by combining the four resonators in HFSS. After the optimization of the responses, the distance s between resonator 1 and 2 (also 3 and 4) is 0.36 mm, between 2 and 3 is 0.5 mm, and between 1 and 4 is 0.9 mm. The simulated insertion loss between 2.4–2.5 GHz is 2.8 dB, and the reflection loss is below −17 dB. The first spurious response is about 12.5 GHz, which is 5 times away from the center frequency, thus it has a good spurious suppression. The whole area of the filter is 12.7 mm × 4.36 mm (about $0.17\lambda_g \times 0.06\lambda_g$), thus having a very compact structure.

4. FABRICATION AND TEST RESULTS

Based on the proposed coupling coefficients and topology structure, a multilayered cross-coupled filter is designed and built. To improve the precision, resonators with inner coupling are printed on the top and bottom side of a Rogers4350B substrate with relative dielectric constant of 3.5 and thickness of 0.254 mm. Then the resonators are laminated on a 0.5 mm substrate to form a 3D multilayered filter as shown in Fig. 7. The measured frequency response, which was obtained using an Anritsu 37369D network analyzer, along with the simulated results are illustrated in Fig. 8. The measured response has a bandwidth of 100 MHz at the center frequency of 2.55 GHz. The insertion loss is 4.5 dB and reflection response is below −10.5 dB. Two transmission zeros are located at 2.45 GHz and 2.72 GHz with over 30 dB rejection. The suppression is below −20 dB from 2.7 GHz to 12 GHz, and the parasitic passband is arisen at 12.5 GHz. Compared

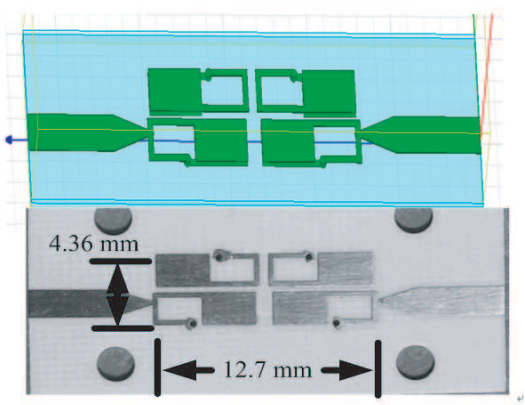

Figure 7. Simulation model of the multilayered filter.

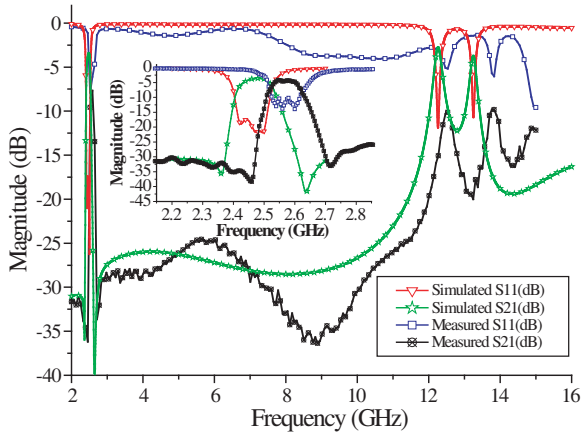

Figure 8. Simulated and test results of the multilayered filter.

with simulation results, the measured center frequency is higher about 100 MHz and the insertion loss is worse than 2 dB. As can be seen, the measured results agree well with the simulated ones, except for some discrepancies in insertion loss and bandwidth of the passband. This is mainly due to the unexpected radiation loss, dielectric loss and fabrication errors, such as substrate warp, stack shift, and line-width variation. Additionally, according to the analysis of the fabrication process, conductor surface roughness is the main reason for the high insertion loss and narrow bandwidths, because bad surface roughness would greatly lower the material conductivity, thus have a great impact on the responses of the passband. Besides, the parasitic effects of the via-holes and unexpected couplings between the stubs could also introduce these discrepancies. Fortunately, this problem can be ameliorated by enhancing the fabrication precision and eliminating unwanted coupling by virtue of HFSS optimization. Further, insertion loss as well as reflection loss can be improved by enhancing Q value of the resonator, which could be achieved by widening the high-impedance stub and lowering the dielectric loss.

5. CONCLUSION

A novel compact cross-coupling 3D resonator, whose size is largely reduced by introducing inner coupling capacitor, is implemented in this paper. Based on the SIR and cross-coupling theory, a four order filter with small size and good stopband rejection is designed and fabricated. Agreement between simulated and measured results

verifies the proposed design. By virtue of its compact size and low cost, the proposed design method and structure could be used in many microwave wireless communication systems to suppress noise and spurious signals. Further, the proposed topology could be easily integrated in many hybrid integrated circuits, such as T/R modules, mobile communication systems and LTCC multilayer circuit modules.

REFERENCES

1. Hong, J. S. and M. J. Lancaster, "Cross-coupled microstrip hairpin-resonator filters," *IEEE Trans. Microwave Theory Tech.*, Vol. 46, 118–122, Jan. 1998.
2. Sagawa, M., K. Takahasi, and M. Makimoto, "Miniaturized hairpin resonator filters and their application to receiver front-end MIC's," *IEEE Trans. Microwave Theory Tech.*, Vol. 37, No. 10, 1991–1997, 1989.
3. Yoon, H. K., Y. J. Yoonjoo, H. Park, and S. Ye, "Hairpin line half wave parallel coupled line narrowband band pass filters using high temperature superconducting thin films," *IEEE Trans. Applied Superconductivity*, Vol. 9, 901–904, Jun. 1999.
4. Kikkert, C. J., "Designing low cost wideband microstrip bandpass filters," *TENCON 2005, IEEE Region 10*, 1–6, Nov. 2005.
5. Hua, L. Z., and K. J. Chen, "A tri-section stepped-impedance resonator for cross-coupled bandpass filters," *IEEE Microwave and Wireless Components Letters*, Vol. 15, No. 6, 401–403, Jun. 2005.
6. Yue, P. Z. and M. Sun, "Dual-band microstrip bandpass filter using stepped-impedance resonators with new coupling schemes," *IEEE Trans. Microwave Theory Tech.*, Vol. 54, No. 10, 3779–3785, Oct. 2006.
7. Zhang, J., J. Z. Gu, B. Cui, and X. W. Sun, "Compact and harmonic suppression open loop resonator bandpass filter with tri-section SIR," *Progress In Electromagnetics Research*, Vol. 69, 93–100, 2007.
8. Pramod, K. S., S. Basu, and Y. H. Wang, "Miniature dual-band filter using quarter wavelength stepped impedance resonators," *IEEE Microwave and Wireless Components Letters*, Vol. 18, No. 2, 88–90, Feb. 2008.
9. Cheng, H. L., C. H. Chen, and C. Y. Chang, "Fabrication-tolerant microstrip quarter-wave stepped-impedance resonator filter," *IEEE Trans. Microw. Theory Tech.*, Vol. 57, No. 5, 1163–1172, May 2009.

10. Wang, Y. X., B. Z. Wang, and J. P. Wang, "A compact square loop dual-mode bandpass filter with wide stop-band," *Progress In Electromagnetics Research*, Vol. 77, 67–73, 2007.
11. Fan, J. W., C. H. Liang, and X. W. Dai, "Design of cross-coupled dual-band filter with equal-length split-ring resonators," *Progress In Electromagnetics Research*, Vol. 75, 285–293, 2007.
12. Zhao, L. P., X. Zhai, B. Wu, T. Su, W. Xue, and C. H. Liang, "Novel design of dual-mode bandpass filter using rectangle structure," *Progress In Electromagnetics Research B*, Vol. 3, 131–141, 2008.
13. Lai, X., Q. Li, P. Y. Qin, B. Wu, and C. H. Liang, "A novel wideband bandpass filter based on complementary split-ring resonator," *Progress In Electromagnetics Research C*, Vol. 1, 177–184, 2008.
14. Lin, W. J., C. S. Chang, J. Y. Li, D. B. Lin, L. S. Chen, and M. P. Houng, "Improved compact broadband bandpass filter using branch stubs co-via structure with wide stopband characteristic," *Progress In Electromagnetics Research C*, Vol. 5, 45–55, 2008.
15. Shobeyri, M. and M. H. Vadjed-Samiei, "Compact ultra-wideband bandpass filter with defected ground structure," *Progress In Electromagnetics Research Letters*, Vol. 4, 25–31, 2008.
16. Wei, F., L. Chen, X.-W. Shi, X. H. Wang, and Q. Huang, "Compact UWB bandpass filter with notched band," *Progress In Electromagnetics Research C*, Vol. 4, 121–128, 2008.
17. Razalli, M. S., A. Ismail, M. A. Mahdi, and M. N. Hamidon, "Novel compact microstrip ultra-wideband filter utilizing short-circuited stubs with less vias," *Progress In Electromagnetics Research*, Vol. 88, 91–104, 2008.
18. Boutejdar, A., A. Elsherbini, A. Balalem, J. Machac, and A. Omar, "Design of new DGS hairpin microstrip bandpass filter using coupling matrix method," *PIERS Proceedings*, 261–265, Prague, Czech Republic, Aug. 27–30, 2007.
19. Weng, L. H., Y. C. Guo, X. W. Shi, and X. Q. Chen, "An overview on defected ground structure," *Progress In Electromagnetics Research B*, Vol. 7, 173–189, 2008.
20. Wang, Z., P. Li, R. Xu, and W. Lin, "A compact X-band receiver front-end module based on low temperature co-fired ceramic technology," *Progress In Electromagnetics Research*, Vol. 92, 157–180, 2009.
21. Rambabu, K. and J. Bornemann, "Simplified analysis technique for the initial design of LTCC filters with all-capacitive coupling,"

IEEE Trans. Microwave Theory Tech., Vol. 53, 1787–1791, May 2005.

22. Kurzrok, R. M., "General three-resonator filters in waveguide," *IEEE Trans. Microwave Theory Tech.*, Vol. 14, 46–47, 1966.
23. Atia, A. E. and A. E. Williams, "Narrow bandpass waveguide filters," *IEEE Trans. Microwave Theory Tech.*, Vol. 4, 258–265, 1972.
24. Cameron, R. J., "General coupling matrix synthesis methods for Chebyshev filtering functions," *IEEE Trans. Microwave Theory Tech.*, Vol. 47, 433–442, Apr. 1999.
25. Cameron, R. J., "Advanced coupling matrix synthesis techniques for microwave filters," *IEEE Trans. Microwave Theory Tech.*, Vol. 51, 1–10, 2003.
26. Mohra, A. S. S., "Compact lowpass filter with sharp transition band based on defected ground structures," *Progress In Electromagnetics Research Letters*, Vol. 8, 83–92, 2009.
27. Chen, X.-Q., R. Li, S.-J. Shi, Q. Wang, L. Xu, and X.-W. Shi, "A novel low pass filter using elliptic shape defected ground structure," *Progress In Electromagnetics Research B*, Vol. 9, 117–126, 2008.
28. Qian, K. and X. Tang, "Compact ultra-wideband low-temperature co-fired ceramic bandstop filter using semi-lumped resonators," *Electromagnetics*, Vol. 32, 193–199, 2012.
29. Xiao, J.-k., S.-W. Ma, S. Zhang, and Y. Li, "Novel compact split ring stepped-impedance resonator (SIR) bandpass filters with transmission zeros," *Journal of Electromagnetic Waves and Applications*, Vol. 21, No. 3, 329–339, 2012.
30. Zhu, Y. Z., H. S. Song, and K. Guan, "Design of optimized selective quasi-elliptic filters," *Journal of Electromagnetic Waves and Applications*, Vol. 23, No. 10, 1357–1366, 2012.
31. Yang, R.-Y., C.-M. Hsiung, C.-Y. Hung, and C.-C. Lin, "A high performance bandpass filter with a wide and deep stopband by using square stepped impedance resonators," *Journal of Electromagnetic Waves and Applications*, Vol. 24, Nos. 11–12, 1673–1683, 2012.
32. AlHawari, A. R. H., A. Ismail, M. F. A. Rasid, R. S. A. R. Abdullah, B. K. Esfeh, and H. Adam, "Compact microstrip bandpass filter with sharp passband skirts using square spiral resonators and embedded-resonators," *Journal of Electromagnetic Waves and Applications*, Vol. 23, Nos. 5–6, 675–683, 2012.